

Surface growth on percolation networks by a conserved-noise restricted solid-on-solid growth model

Sang Bub Lee*

*Department of Physics and Department of Nano-Science & Technology of Graduate School,
Kyungpook National University, Daegu 41566, Korea*

(Received 18 September 2015; revised manuscript received 13 November 2015; published 11 February 2016)

Surface growth by the conserved-noise restricted solid-on-solid model is investigated on diluted lattices, i.e., on percolation networks that are embedded in two spatial dimensions. The growth exponent β and the roughness exponent α are defined, respectively, by the mean-square surface width via $W^2(t) \sim t^{2\beta}$ and the mean-square saturated width via $W_{\text{sat}}^2(L) \sim L^{2\alpha}$, where L is the system size. These are measured on both an infinite network and a backbone network and the results are compared with power-counting predictions obtained using the fractional Langevin equation. While the Monte Carlo results on deterministic fractal substrates show excellent agreement with the predictions [D. H. Kim and J. M. Kim, *Phys. Rev. E* **84**, 011105 (2011)], the results on critical percolation networks deviate by 8%–12% from these predictions.

DOI: [10.1103/PhysRevE.93.022118](https://doi.org/10.1103/PhysRevE.93.022118)

I. INTRODUCTION

During the past few decades, there has been a considerable effort to elucidate the growth dynamics of roughening surfaces using various discrete growth models [1–4]. Surface-roughening phenomena are associated with a wide variety of systems such as domain walls in the two-dimensional random bond Ising model [5], randomly stirred fluids, ballistic aggregation [6], epitaxial film growth [7], and directed polymers in a random potential [8].

Various continuum equations were proposed in order to classify growth phenomena into several distinct universality classes. The growth phenomena are classified by the critical exponents that characterize the growth of the surface width in a large system and the saturated width in finite-size systems. The growing surface width in a system of a linear size L is defined by the standard deviation of the surface heights, given as

$$W(t, L) = \langle [h(\vec{r}, t) - \overline{h(t)}]^2 \rangle^{1/2}, \quad (1)$$

where $\overline{h(t)}$ is the average height over all lattice sites at time t and $\langle \dots \rangle$ denotes the average over all samples. For finite t and L , the mean-square surface width satisfies the scaling function

$$W^2(L, t) = L^{2\alpha} \mathcal{F}(t/L^z) \propto \begin{cases} t^{2\beta}, & t \ll L^z \\ L^{2\alpha}, & t \gg L^z, \end{cases} \quad (2)$$

where the extreme values are given as $\mathcal{F}(x) = \text{const}$ for $t \gg L^z$ and $\mathcal{F}(x) \propto x^{2\beta}$ for $t \ll L^z$ and β and α are the growth and roughness exponents, respectively. The dynamic exponent z is defined by $z = \alpha/\beta$.

The most prominent universality class is the Kardar-Parisi-Zhang (KPZ) class in which the growth is believed to be described by a continuum equation, known as the KPZ equation [9],

$$\frac{\partial h(\vec{r}, t)}{\partial t} = \nu \nabla^2 h(\vec{r}, t) + \frac{\lambda}{2} [\nabla h(\vec{r}, t)]^2 + \eta(\vec{r}, t), \quad (3)$$

where η represents the Gaussian random variable that satisfies

$$\langle \eta(\vec{r}, t) \eta(\vec{r}', t') \rangle = 2\Gamma \delta(\vec{r} - \vec{r}') \delta(t - t'), \quad (4)$$

with Γ describing the local noise variation. Various discrete models that differ greatly from each other, such as the Eden model [10], ballistic deposition [11], and restricted solid-on-solid (RSOS) model [12], can all be described by the KPZ equation and, accordingly, these models are considered to belong to the KPZ universality class. There are other known universality classes, such as the Edwards-Wilkinson (EW) class [13] described by the EW equation

$$\frac{\partial h(\vec{r}, t)}{\partial t} = \nu \nabla^2 h(\vec{r}, t) + \eta(\vec{r}, t) \quad (5)$$

and the Herring-Mullins (HM) class [14,15], all of which have been studied on pure substrates.

In each of these models, the number of particles on a substrate is not conserved because of either deposition or evaporation or both processes. Recently, a growth model with a conserved number of particles was also presented and studied on both a regular lattice [16–18] and selected fractal substrates [19]. It is known that particle conservation on a substrate leads to a conserved noise, described by [16]

$$\langle \eta_c(\vec{r}, t) \eta_c(\vec{r}', t') \rangle = -2D_c \nabla^2 \delta^d(\vec{r} - \vec{r}') \delta(t - t'), \quad (6)$$

where D_c is the noise variation. Therefore, the RSOS model with particle conservation is referred to as the conserved-noise RSOS (CNR SOS) model.

Growth in the CNRSOS model is described by the continuum Langevin equation [16,18]

$$\frac{\partial h(\vec{r}, t)}{\partial t} = -\nu \nabla^4 h(\vec{r}, t) + \eta_c(\vec{r}, t), \quad (7)$$

which is a form of the HM equation, but with a conserved noise. The critical exponents can be obtained exactly through a simple power-counting method when the size of a system is rescaled by a factor b , i.e., $h \rightarrow b^\alpha h$, $t \rightarrow b^z t$, and $\eta_c \rightarrow b^{-(2+d+z)/2} \eta_c$,

$$\alpha = \frac{2-d}{2}, \quad \beta = \frac{2-d}{8}, \quad z = 4, \quad (8)$$

where d is the substrate dimension (note that the total dimension is equal to $d+1$).

These growth phenomena have recently been studied on various fractal lattices [20–27]. On a given fractal substrate, the linear continuum equation for the CNRSOS model was

*sblee@knu.ac.kr

modified by replacing $\nabla^4 h$ with $\nabla^{2z_{rw}} h$ and the fractional Langevin equation was obtained [19]. The main idea for this modification was borrowed from the EW equation [21]. From power counting of the left-hand term and the first term on the right-hand side of Eq. (5), the dynamic exponent $z = 2$ results from the order of ∇ . Because the EW equation without noise is equivalent to the diffusion equation, the value of z is the dynamic exponent of random walks z_{rw} , defined by the mean-square end-to-end distance $\langle R^2 \rangle \sim t^{2/z_{rw}}$. On a regular lattice, $z_{rw} = 2$, irrespective of the substrate dimensions; however, on a fractal substrate, anomalous diffusion yields the fractional number z_{rw} . Substituting $\nabla^2 \rightarrow \nabla^{z_{rw}}$ in Eq. (5), the fractional EW equation is obtained and power counting of the rescaling factors yields the growth and roughness exponents

$$\alpha_{EW} = d_f \left(\frac{1}{d_s} - \frac{1}{2} \right), \quad \beta_{EW} = \frac{1}{2} \left(1 - \frac{d_s}{2} \right). \quad (9)$$

The results in Eq. (9) were also obtained previously by direct calculation of the surface width using the autocorrelation function on fractal substrates [28] and they were found to be in excellent agreement with the Monte Carlo (MC) data on deterministic fractal substrates [21] and also on random fractal substrates [22].

For the fourth-order HM equation, the continuum Hamiltonian written as $H \sim \int d^d x |\frac{\nabla^2 h}{N}|^2$ leads to the fourth-order differential equation. Thus, from the analogy between the EW equation and the HM equation, it is not unreasonable to replace $\nabla^4 h$ with $\nabla^{2z_{rw}} h$ and the fractional Langevin equation

$$\frac{\partial h(\vec{r}, t)}{\partial t} = -v \nabla^{2z_{rw}} h(\vec{r}, t) + \eta_c(\vec{r}, t) \quad (10)$$

was proposed [19] with the conserved noise modified in order to satisfy

$$\langle \eta_c(\vec{r}, t) \eta_c(\vec{r}', t) \rangle = -2D_c \nabla^2 \delta^{dt}(\vec{r} - \vec{r}') \delta(t - t'), \quad (11)$$

where d_f is the substrate fractal dimension. Through power counting of the rescaling factors, the following critical exponents were obtained:

$$\alpha = \frac{z_{rw} - d_f}{2}, \quad \beta = \frac{1}{4} - \frac{d_f}{4z_{rw}}, \quad z = 2z_{rw}. \quad (12)$$

Using the scaling relation $z_{rw} = d_w = \frac{2d_f}{d_s}$ for random walks on a fractal substrate [29], Eq. (12) can be rewritten as

$$\alpha = d_f \left(\frac{1}{d_s} - \frac{1}{2} \right), \quad \beta = \frac{1}{4} \left(1 - \frac{d_s}{2} \right), \quad z = 2d_w, \quad (13)$$

where d_w and d_s are the fractal dimension of the random walk and the spectral dimension of the substrate, respectively. The predictions obtained using Eq. (13) are in excellent agreement with the MC results on the Sierpinski gasket and checkerboard fractal substrates and, based on the numerical results, they were conjectured to be exact on fractal substrates [19].

In this paper the CNRSOS growth model is studied on diluted lattices, i.e., on percolation networks, in order to examine the validity of Eq. (13) on random fractal substrates. The growth phenomena on diluted lattices may differ from the growth on deterministic fractal substrates. As an example, while the growth by the RSOS model on deterministic fractal substrates yields distinct critical behaviors with well-defined critical exponents [20], that on diluted lattices, i.e.,

on percolation networks, results in anomalous nonuniversal growth [22]. Therefore, the agreement of the predictions in Eq. (13) with the MC data on two selected deterministic fractal substrates does not warrant similar agreement for the random fractal substrates. Growth on diluted lattices is of interest in two respects. First, it enables one to explore the influence of quenched impurities on growth dynamics because diluted sites are generally considered to be quenched impurities. Investigation of the influence of quenched impurities has been of great interest in both equilibrium and nonequilibrium critical phenomena since the discovery of the Harris criterion [30]. In the nonequilibrium RSOS model, quenched impurities were found to be relevant and even small amounts of impurities yielded nonuniversal anomalous growth. In the equilibrium RSOS growth, however, the presence of impurities was irrelevant and regular lattice results were observed as long as the amount of impurities was less than a critical amount [22]. It is thus interesting to investigate the way in which impurity sites affect growth in the CNRSOS model. Second, one can also examine whether the fractional Langevin equation that was obtained by such a crude method is also able to predict growth on random fractal lattices. Because the growth exponent β was predicted to depend only on the spectral dimension of the substrate, the growth exponents on two- and three-dimensional critical percolation networks and on a backbone network are expected to be similar, because the spectral dimensions for these networks are similar. Growth on these substrates is investigated.

In Sec. II the model and simulation methods are described. In Sec. III the MC results are presented and discussed. A summary and conclusion are presented in Sec. IV.

II. MODEL AND METHOD

The random fractal lattice, i.e., the percolation network, is generated on a square lattice of a linear size L using the standard method; each lattice site is occupied with a probability p and diluted with a probability $1 - p$ and any two occupied nearest-neighbor sites are assumed to be connected. An infinite network is sampled using periodic boundary conditions; a cluster that spans all the coordinate directions and is wrapped around the system using periodic boundaries is considered to be the random fractal substrate, so the substrate should be indefinitely extendable when periodically replicated. The well-known Hoshen-Kopelman algorithm was employed here [31]. At each occupied lattice site, the number of and directions to occupied nearest-neighbor sites are recorded in terms of a single integer variable, with the fifth digit representing the number of occupied sites and the following four digits representing the directions. As an example, the integer 30 421 represents the fact that the neighboring sites along the $+x$, $-x$, and $-y$ directions are occupied and that there are three occupied nearest-neighbor sites. The percolation backbone is extracted using the Roux-Hansen algorithm [32], which is very efficient but effective only in two dimensions.

The growth rule of the CNRSOS model is to randomly select a nearest-neighbor pair of occupied sites (\vec{r}_i, \vec{r}_j) . A particle on site \vec{r}_i is then moved to site \vec{r}_j , resulting in

$$h(\vec{r}_i) \rightarrow h(\vec{r}_i) - 1, \quad h(\vec{r}_j) \rightarrow h(\vec{r}_j) + 1,$$

or vice versa, resulting in

$$h(\vec{r}_i) \rightarrow h(\vec{r}_i) + 1, \quad h(\vec{r}_j) \rightarrow h(\vec{r}_j) - 1,$$

with equal probabilities. The RSOS condition

$$|h(\vec{r}_i, t) - h(\vec{r}_j, t)| \leq N \quad (14)$$

is examined and, if this is not satisfied for any of the sites at \vec{r}_i and \vec{r}_j or their nearest-neighbor sites, the corresponding local movement is forbidden and the particle remains in its original position. Because no deposition or evaporation except surface diffusion is allowed, the sum of the heights $\sum_i h(\vec{r}_i)$ is conserved and therefore $\bar{h}(t) = 0$, assuming that the surface grows from a flat substrate. At each attempt, the evolution time is increased by $\Delta t = 1/N_{\text{occu}}$, where N_{occu} is the number of occupied sites, and the surface width is recorded whenever an evolution time exceeds integer values. A single surface is grown on each sampled percolation network and the results are averaged over many uncorrelated networks.

III. RESULTS AND DISCUSSION

In order to examine whether diluted sites affect the growth dynamics, simulations were carried out on a square lattice for $p = 1.0, 0.8$, and 0.7 , all of which were above the percolation threshold $p_c = 0.592745$ [33]. Simulations on an infinite network and on a backbone network, both at p_c , were also carried out in order to investigate growth dynamics on random fractal substrates. The RSOS condition was set to an integer value of $N = 3$ throughout the simulations. It should be noted that larger values of N yielded faster growth with the same critical exponents; however, the power-law region narrowed for larger N values.

A. Growth on a percolation network for $p > p_c$

Figure 1 shows the mean-square surface width plotted on a semilogarithmic scale. For $p = 1.0$, the substrate is a flat square lattice and the surface width grows logarithmically, as one would expect at the critical dimension. From Eq. (8), the critical dimension of the CNRSOS model is predicted to be $d_c = 2$ because $\alpha = \beta = 0$ for $d = 2$. The simulation results support this prediction. For $p = 0.8$ and 0.7 , the surface width increases rapidly in the early growth stages and increases logarithmically later on. The rapid increase in the early stages is attributed to the local fractal nature of the substrates, whereas with increasing time, the global Euclidean structure dominates the growth. The region of logarithmic increase becomes narrower with increasing p . It is expected that this region would disappear at $p = p_c$, with the growth eventually following a power-law behavior, as described in the following section.

On the upper critical dimension, the surface width is known to satisfy the scaling form

$$W^2(L, t) = \log_{10} \left[L^{2a} \mathcal{G} \left(\frac{t}{L^z} \right) \right] \propto \begin{cases} 2b \log_{10} t, & t \ll L^z \\ 2a \log_{10} L, & t \gg L^z, \end{cases} \quad (15)$$

where the scaling function is given by $\mathcal{G}(x) \propto x^{2b}$ for $x \ll 1$ and $\mathcal{G}(x) = \text{const}$ for $x \gg 1$. In order to examine the scaling of the data provided in Fig. 1, the values of (b, a) are estimated to be $(0.280, 1.119)$ for $p = 1.0$, $(0.606, 2.292)$ for $p = 0.8$, and

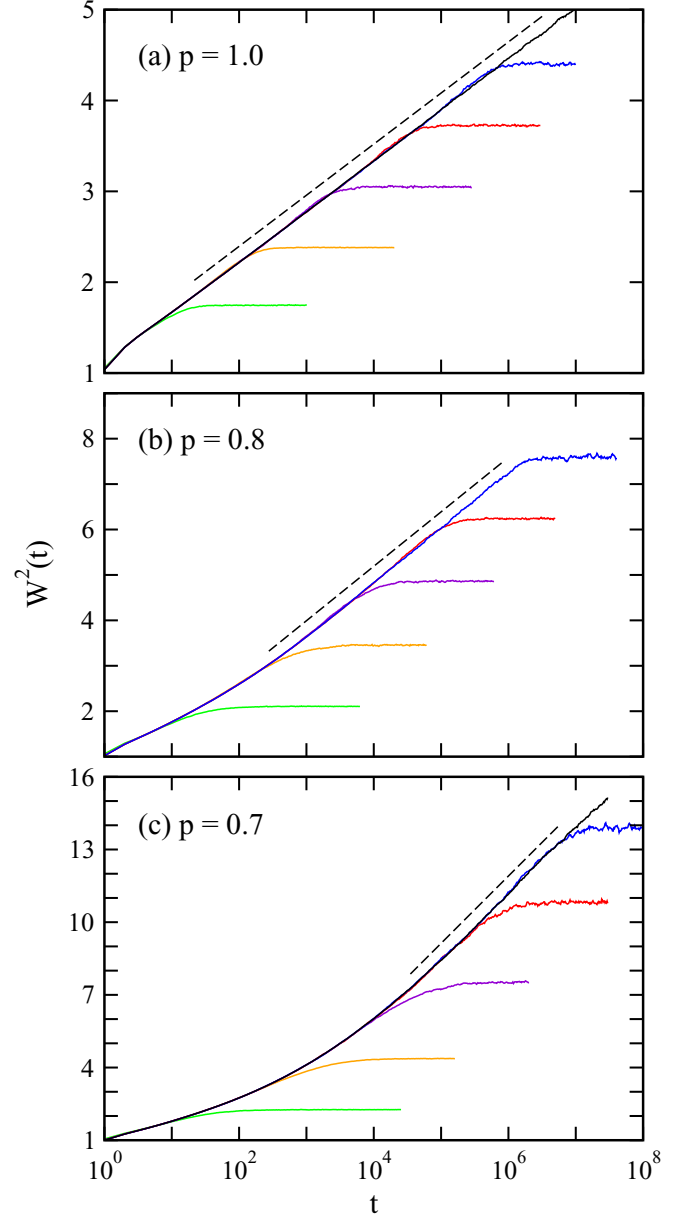


FIG. 1. Mean-square width of the growing surfaces calculated using the CNRSOS model on a percolation network for three selected values of percolation probability: (a) $p = 1.0$, (b) $p = 0.8$, and (c) $p = 0.7$. The data in each plot are for, from bottom to top, $L = 4, 8, 16, 32, 64$, and 256 and the dashed line is a guide for the eye, denoting a logarithmic increase.

$(1.397, 5.302)$ for $p = 0.7$. From the scaling form in Eq. (15), the dynamic exponent is given as $z = \frac{a}{b}$ and from the estimates of b and a , $z = 4.0$ for $p = 1.0$ and $z \simeq 3.8$ for both $p = 0.8$ and 0.7 . The slight deviation of the latter from the value of the former appears to be due to a crossover from fractal-like to Euclidean substrate behaviors with increasing time.

Scaling plots of the data for $p = 1.0$ and 0.8 are shown in Fig. 2, using the estimated values of a and z . In the case of $p = 1.0$, the scaling is perfect, implying that indeed $d_c = 2$. This scaling plot is precisely the same as that of Ref. [18], except that the value of a in this work is slightly larger. In the

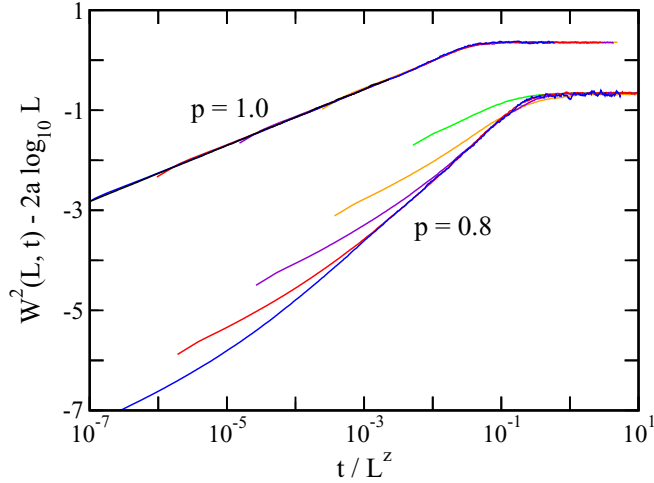


FIG. 2. Scaling plots of Eq. (15), using the estimated values of $2\alpha = 2.238$ and $z = 4.0$ for $p = 1.0$ (upper) and $2\alpha = 4.584$ and $z = 3.8$ for $p = 0.8$ (lower), for the CNRSOS model on a percolation network above p_c .

case of $p = 0.8$, data in the early stages deviate and merge into a single curve as time increases, reflecting the crossover from fractal-like to Euclidean logarithmic growth. The case of $p = 0.7$ shows similar results, but with a narrower logarithmic growth region (not shown).

B. Growth on random fractal lattices

At the percolation threshold, an infinite percolation network becomes fractal, with the fractal dimension $d_f = \frac{91}{48} \simeq 1.896$ [34], in the two embedding dimensions. The growth dynamics on an infinite network is thus expected to be distinct from that on a regular lattice substrate. The snapshots in Fig. 3 show the growth on two different substrates with $L = 32$, i.e., for $p = 1.0$ (regular square lattice) and for $p = p_c$ (critical percolation network), at times, from top to bottom, $t = 10, 10^2, 10^3, 10^4, 10^5$, and 10^6 . The surface width on a regular lattice grows slowly, whereas that on a critical percolation network shows faster growth. (Note that the ungrown flat sites for $p = p_c$ are the diluted sites and the growth on the sites neighboring the diluted sites is distinct because of fewer restrictions.)

The mean-square surface width was calculated on infinite percolation networks. Figure 4 shows the mean-square surface width for selected system sizes of $L = 4, 8, 16, 32, 64$, and 256 . In the case of $L = 64$, the data do not reach the steady-state value after 10^9 steps because of extremely slow convergence behavior, indicating that the dynamic exponent is much larger than that on a regular lattice. A crude estimation of the saturation time gives $t_s \sim L^z \approx 10^{11}$ for $L = 64$ and $z = 6$ (see below). For $L = 256$, data were generated up to 10^7 MC steps in order to accurately estimate the growth exponent; it was determined from power-law fitting that $2\beta = 0.188(1)$. The saturated mean-square surface width versus system size is provided in the inset; power-law fitting yields a value of $2\alpha = 1.122(5)$. In order to validate these estimates, the scaling function is plotted in Fig. 5, using the estimated values of $2\alpha = 1.122$ and $z = \frac{\alpha}{\beta} = 5.97$. From this figure, it is clear that the scaled surface width for various-size systems collapses

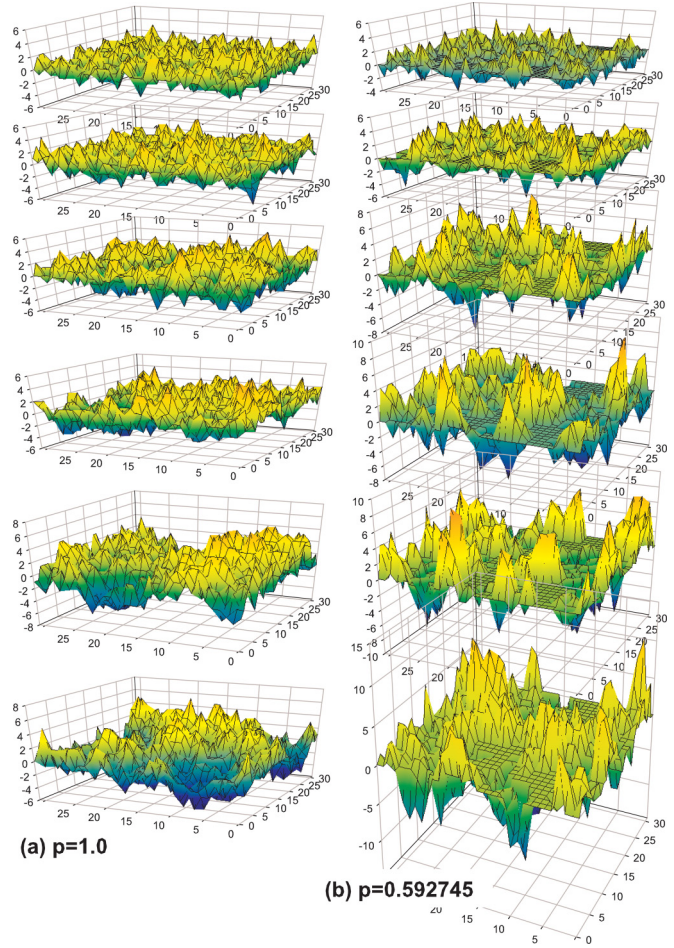


FIG. 3. Snapshots of the growing surfaces by the CNRSOS model on a lattice of $L = 32$ for (a) $p = 1.0$ and (b) $p = 0.592745 (= p_c)$, at the time steps of, from top to bottom, $t = 10, 10^2, 10^3, 10^4, 10^5$, and 10^6 .

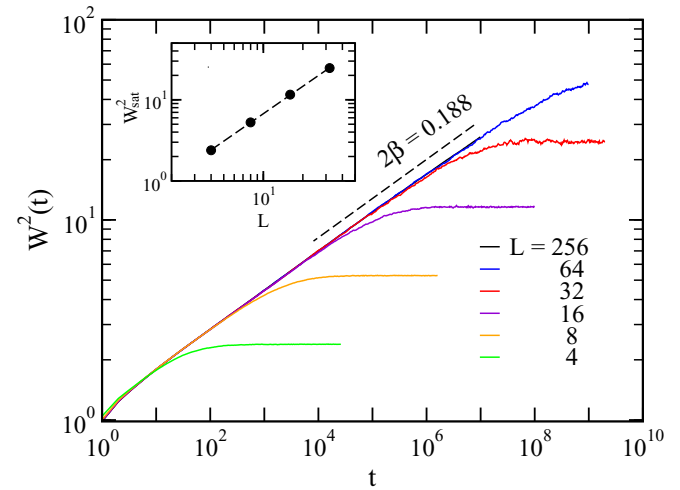


FIG. 4. Mean-square surface width generated by the CNRSOS model on a critical percolation network for system sizes of, from bottom to top, $L = 4, 8, 16, 32, 64$, and 256 (up to 10^7 steps). The inset is a plot of the mean-square saturated width as a function of the system size, with a regression fit yielding $2\alpha = 1.122$.

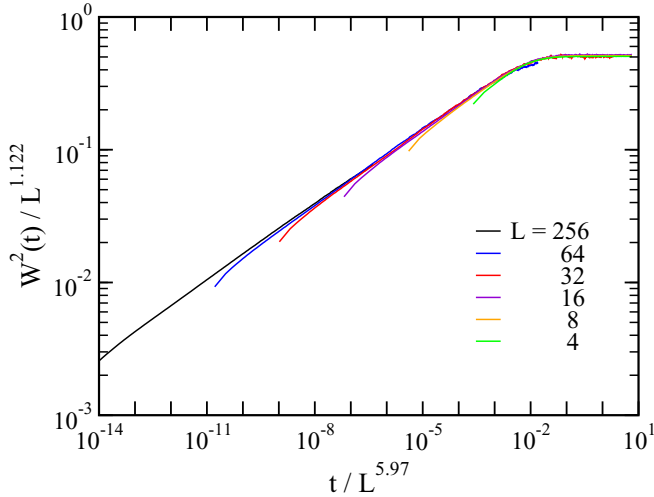


FIG. 5. Scaling plot of Eq. (2) using the estimated values of $2\alpha = 1.122$ and $z = 5.97$ for the CNRSOS model on a critical percolation network.

onto a single curve when plotted as a function of the scaled variable. This confirms that the estimates are valid.

Simulations were also carried out on percolation backbone networks that were obtained from infinite networks by eliminating all dangling bonds and blobs. Because all dangling ends were eliminated from the infinite network that was generated at p_c , the backbone network is a fractal with a fractal dimension smaller than that of the original infinite network, $d_f^{bb} \simeq 1.64$ [35,36]. The spectral dimension, on the other hand, remains unchanged. The spectral dimension, also referred to as the fracton dimension, is originally defined by the density of normal modes on fractal lattices as $\rho(\omega) \sim \omega^{d_s-1}$ [37] and is also related to the probability of random walks returning to the origin after t steps, $P(t) \sim t^{-d_s/2}$ [29]. Because dangling ends do not contribute to lattice vibration, the spectral dimension of a backbone is the same as that of an infinite network.

In Fig. 6 the mean-square surface widths generated on backbone networks for systems of $L = 4, 8, 16, 32, 64,$ and 512 are plotted. Comparing this plot with Fig. 4, it is clear that the surface width saturates faster and the saturated width is smaller than the growth on an infinite network. This result is expected when the mean coordination number on a backbone network is larger than that on an infinite network. Indeed, the mean coordination number is larger on a backbone network because all the dangling sites with fewer occupied neighboring sites are eliminated from the infinite network and, accordingly, growth is more restricted on a backbone than on an infinite network when using the RSOS condition. The estimated exponents are $2\beta = 0.186(2)$, $2\alpha = 0.977(5)$, and $z \simeq 5.25(6)$. Data scaled using these values yields excellent collapse, as shown in Fig. 7.

The results are summarized in Table I, with a comparison to the power-counting predictions obtained using the fractional Langevin equation, using $d_s = 1.31$, $d_f = \frac{91}{48}$ [29], and $d_w = 2.87$ [29,38] for the data on an infinite network and $d_f^{bb} = 1.64$ [35,36] and $d_w = 2.69$ [29] for the data on a backbone network. The measured values of β and α are larger than the predicted values by approximately 8%–12%, in contrast to the results obtained on deterministic fractal substrates [19].

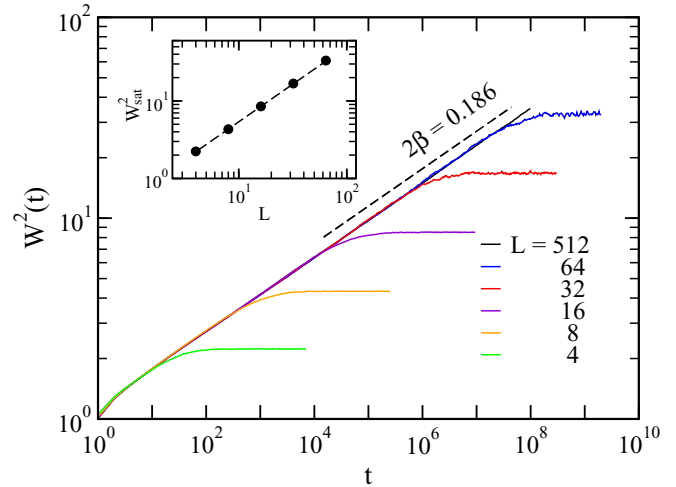


FIG. 6. Mean-square surface width generated using the CNRSOS model on a percolation backbone network for, from bottom to top, $L = 4, 8, 16, 32, 64,$ and 512 . The dashed line is the power-law fit of the data for $L = 512$ and the saturated width as a function of the size of system is provided in the inset, with a regression fit yielding $2\alpha = 0.977$.

C. Discussion

In the case of $p = 0.7$ and 0.8 , the growth of surface width differs only in the early stages and it recovers to a logarithmic increase in the long-time region, indicating that quenched impurities have no effect on critical behavior as long as the amount of impurities present is less than the critical amount and that the upper critical dimension of the CNRSOS model is 2, as predicted by Eq. (8). On the other hand, for the case of $p = p_c$, the MC data of the critical exponents deviate by approximately 8%–12% from the predictions of the fractional Langevin equation. Because the power-counting predictions of Eq. (13) agree well with the critical exponents for growth on two typical deterministic fractal substrates,

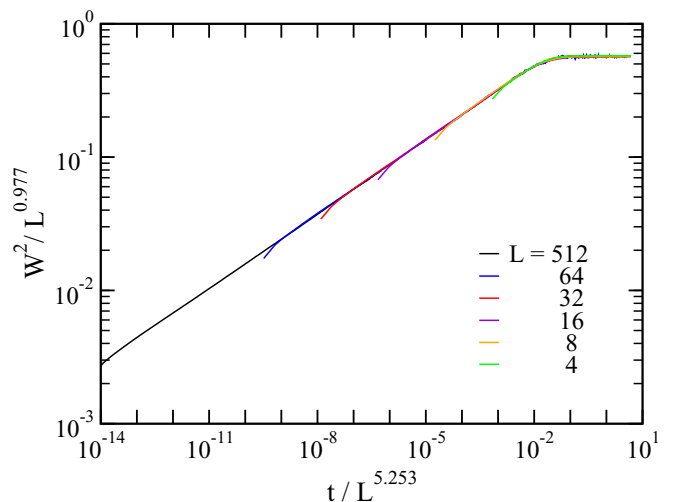


FIG. 7. Scaling plot of the surface width on a percolation backbone network, generated using the CNRSOS model. Data scaled using the estimated values of α and z yield perfect scaling.

TABLE I. Summary of the critical exponents for the CNRSOS model on percolation networks, in comparison with power-counting predictions obtained using the fractional Langevin equation.

Critical exponents	β	α	z
On infinite network:			
MC estimates	0.094(1)	0.561(3)	5.97(6)
Eq. (13) ^a	0.0863	0.499	5.74
On backbone network:			
MC estimates	0.093(1)	0.489(3)	5.25(6)
Eq. (13) ^b	0.0863	0.432	4.95

^acalculated using $d_s = 1.31$, $d_f = \frac{91}{48}$ [29], and $d_w = 2.87$ [29,38].

^bcalculated using $d_f^{bb} = 1.64$ [35,36] and $d_w = 2.69$ [29].

one may also anticipate similar results on random fractal substrates. However, the MC results obtained in this work are at variance with this expectation.

In order to elucidate the reasons for this discrepancy, possible sources of errors are discussed in this section. First, on random fractal lattices, the averaging procedure has been an issue for the problem of self-avoiding walks [39,40]. The correct averaging procedure has been known to consist of two steps, i.e., averaging over many conformations on a given disorder and then averaging over many disorder configurations, and researchers have claimed that incorrect averaging procedures yield wrong critical behaviors. Taken from an analogy between self-avoiding walks and surface growth, additional simulations were carried out for selected values of L at p_c , averaging over 100 different growth conformations on a given percolation network and then over 100 uncorrelated percolation networks. It was found that after carrying out sufficient disorder averages the two results were indistinguishable; in addition, the convergence behavior of the results of this work was much faster.

Second, because roughness and dynamic exponents are associated with the fractal dimensions of random walks, the convergence behavior of the growing surfaces might depend on the dynamic procedures, as for random walks problem. Two typical models for generating random walks, the blind ant and myopic ant models, were proposed on disordered media [29]. While a myopic ant hops to a neighboring occupied site at every step, a blind ant may stay or hop with probabilities that depend on the local connectivity, with time increased for both cases. It was found that the blind ant yielded the asymptotic results of the mean square end-to-end distances much faster than the myopic ant did. For the surface growth, because the neighboring pairs of occupied sites were selected, the method employed in this work corresponds to the myopic ant description of random walk. In order to examine if slow convergence of the surface width toward the asymptotic behavior might have caused a systematic error, the blind ant description was also designed in the following manner. An occupied site was first selected and then a neighboring site was selected from its four nearest-neighbor sites with equal probabilities and if an unoccupied site was selected, the current trial was forbidden but evolution time was increased. The MC data exhibited growth that was delayed by $\Delta(\log_{10} t) \approx 0.2$ and both the growth and roughness exponents remained unchanged.

Finally, because relatively small systems were used in the growth simulations, the local structures of the small percolation networks may not have behaved like fractals and the growth on such small systems may not have correctly reflected fractal substrate results. This might be the most likely source of any systematic errors. However, considering that systems of the same size generated by the same method as in this work did not lead to discrepancies in the growth using the equilibrium RSOS model on a percolation network [22], this is less likely in the case of the CNRSOS model. Moreover, the growth exponents that were measured on relatively large systems of $L = 256$ for an infinite network and $L = 512$ for a backbone network were larger by more than 8% than the predictions. In addition, because small systems generated using the periodic boundary condition are known to be more compact than any subset of a larger system or of an infinite system, growth is suppressed to a greater degree on a smaller system when using the RSOS condition and, accordingly, the growth and roughness exponents should become smaller. Therefore, if the use of small systems caused a systematic error, the discrepancy due to system sizes would have been in the opposite direction.

Considering this discussion, the discrepancy does not appear to be due to the systematic error but is instead attributable to the poor predictions of the fractional Langevin equation. Therefore, the fractional Langevin equation obtained by a simple replacement of $\nabla^4 \rightarrow \nabla^{2z_w}$ may not describe the growth dynamics as well as it does for the growth on deterministic fractal substrates and the prediction of the exponent values appears not to be exact for the growth using the CNRSOS model on random fractal substrates. This result is also in contrast to that of the equilibrium RSOS model, in which the predictions from the fractional EW equation are in excellent agreement with the MC data.

What then makes the agreement between the predicted exponents and MC data different for the equilibrium RSOS model and the CNRSOS model? In order to understand the difference, it is necessary to look into the results of the equilibrium RSOS model. As mentioned in Sec. I, the exponents in Eq. (9) were first derived rigorously by a direct integration of Eq. (5) on fractal substrates [28]. The authors of Ref. [21] obtained later the same results by a simpler method of power counting for the scaling factor in the fractional EW equation. Whether the same power-counting method using the fractional HM equation gives the results that can be obtained by a direct integration of the fourth-order HM equation with a conserved noise remains to be resolved in order to validate Eq. (13) for the growth by the CNRSOS model. A full understanding of the discrepancy between the predictions and MC data is expected to follow.

D. Comparison of growth in two and three dimensions

The continuum fractional Langevin equation predicts that the roughness and dynamic exponents on infinite networks are larger than those on backbone networks because $d_f > d_f^{bb}$ and $d_w > d_w^{bb}$. The growth exponent β , on the other hand, is similar for the two cases because it depends only on the spectral dimension. These predictions are qualitatively consistent with the simulation results. One may then ask

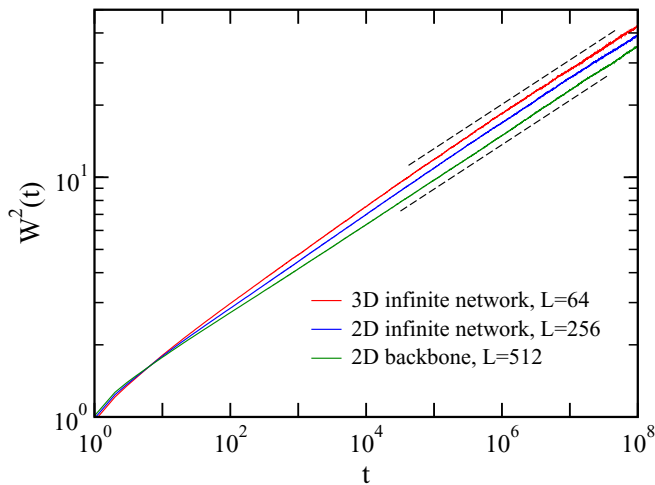


FIG. 8. Mean-square surface widths obtained by the CNRSOS model on infinite percolation networks in two dimensions (middle blue) and three dimensions (top red) and on a percolation backbone network (bottom green), generated at p_c . The two dashed lines of the same power are provided as a guide for the eye.

whether the growth exponent on a three-dimensional infinite network is similar to that on a two-dimensional network. This question originates from a conjecture proposed by Alexander and Orbach [37], who suggested that $d_s = \frac{4}{3}$ on percolation networks, irrespective of the embedding dimension. Although this conjecture was refuted through accurate examination [41,42], the values of d_s that were obtained were found to be similar within 5%.

Simulations on an infinite network that was generated for $p_c = 0.3117$ [43] in three embedding dimensions were performed. However, because $d_w \simeq 3.7$ [29] and, accordingly, $z \approx 7.5$, the surface width saturated extremely slowly and estimation of the roughness exponent was not possible. Therefore, only the growth exponent was measured on the network with $L = 64$. The results are compared with those on an infinite network and on a backbone network in Fig. 8. Although initially the increase in surface width differs, the powers of the growing surface widths for the three cases become similar with increasing time, supporting the predictions of Eq. (13) that

the growth exponents depend only on the spectral dimension of the substrate.

IV. SUMMARY AND CONCLUSION

In summary, surface growth by the CNRSOS model was studied using MC simulations on random fractal substrates, i.e., on infinite percolation networks and on backbone networks, both embedded in two dimensions. For $p > p_c$, the surface width increased logarithmically with time and the saturated width also increased in a similar manner with increasing system size, indicating that $\beta = \alpha = 0$. The MC data exhibited perfect scaling for $p = 1$, while the data for $p = 0.8$ and 0.7 yielded a crossover from a power-law increase to a logarithmic divergence with increasing time. For $p = p_c$, the power-law increase of the surface width was observed on both infinite and backbone networks, with similar growth exponents of $\beta \simeq 0.094$. The roughness and dynamic exponents were found to differ by approximately 15% for these two cases. The growth exponent was predicted to be similar for the growth on infinite percolation networks in both two and three dimensions as well as on the backbone network and the MC data were in agreement with the prediction.

The estimated exponents were compared with power-counting predictions obtained using the fractional Langevin equation. The estimates of the MC data were larger than the predicted values by approximately 8%–12%. It is therefore concluded that the proposed fractional Langevin equation that involves a simple replacement of ∇^4 with $\nabla^{2z_{\text{rw}}}$ does not appear to describe growth dynamics on random fractal substrates as well as it does on deterministic fractal substrates, for the growth using the CNRSOS model. Possible sources of the discrepancy were discussed, although a full understanding of these results requires further research. A direct integration of the fourth-order HM equation with a conserved noise might be one of the possible solutions.

ACKNOWLEDGMENTS

The author thanks J. M. Kim at Sungsil University for discussions and is grateful for the hospitality of the Department of Chemistry, Princeton University, where part of this work was performed. This research was supported by the Kyungpook National University Research Fund. The author is grateful for this financial support.

-
- [1] *Dynamics of Fractal Surfaces*, edited by F. Family and T. Vicsek (World Scientific, Singapore, 1991).
 - [2] J. Krug and H. Spohn, in *Solids Far From Equilibrium: Growth, Morphology and Defects*, edited by C. Godreche (Cambridge University Press, New York, 1991).
 - [3] T. Vicsek, *Fractal Growth Phenomena* (World Scientific, Singapore, 1992).
 - [4] A.-L. Barabási and H. E. Stanley, *Fractal Concepts in Surface Growth* (Cambridge University Press, Cambridge, 1995).
 - [5] D. A. Huse and C. L. Henley, Pinning and roughening of domain walls in Ising systems due to random impurities, *Phys. Rev. Lett.* **54**, 2708 (1985).
 - [6] J. M. Burgers, *The Nonlinear Diffusion Equation* (Reidel, Boston, 1974).
 - [7] A. Pimpinelli and J. Villain, *Physics of Crystal Growth* (Cambridge University Press, Cambridge, 1998), and references therein.
 - [8] M. J. Vold, A numerical approach to the problem of sediment volume, *J. Colloid Sci.* **14**, 168 (1959).
 - [9] M. Kardar, G. Parisi, and Y. C. Zhang, Dynamic scaling of growing interfaces, *Phys. Rev. Lett.* **56**, 889 (1986).
 - [10] R. Jullien and R. Botet, Surface thickness in the Eden model, *Phys. Rev. Lett.* **54**, 2055 (1985).
 - [11] P. Meakin, P. Ramanlal, L. M. Sander, and R. C. Ball, Ballistic deposition on surfaces, *Phys. Rev. A* **34**, 5091 (1986).
 - [12] J. M. Kim and J. M. Kosterlitz, Growth in a restricted solid-on-solid model, *Phys. Rev. Lett.* **62**, 2289 (1989); J. M. Kim, J. M. Kosterlitz, and T. Ala-Nissila, Surface growth and crossover

- behavior in a restricted solid-on-solid model, *J. Phys. A* **24**, 5569 (1991).
- [13] S. F. Edwards and D. R. Wilkinson, The surface statistics of a granular aggregate, *Proc. R. Soc. London A* **381**, 17 (1982).
- [14] C. Herring, Effect of change of scale on sintering phenomena, *J. Appl. Phys.* **21**, 301 (1950).
- [15] W. W. Mullins, Theory of thermal grooving, *J. Appl. Phys.* **28**, 333 (1957).
- [16] J. M. Kim, The relation between conserved noise restricted solid-on-solid model and restricted curvature model, *Mod. Phys. Lett. B* **18**, 11 (2004).
- [17] J. M. Kim and D. H. Kim, Conserved noise restricted curvature model, *J. Stat. Phys.* **131**, 1179 (2008).
- [18] J. H. Lee, D. H. Kim, and J. M. Kim, Solid-on-solid model with conserved noise in higher dimensions, *J. Korean Phys. Soc.* **53**, 1797 (2008).
- [19] D. H. Kim and J. M. Kim, Conserved noise restricted-solid-on-solid model on fractal substrates, *Phys. Rev. E* **84**, 011105 (2011).
- [20] S. B. Lee, H.-C. Jeong, and J. M. Kim, A restricted solid-on-solid model for growth on fractal substrates, *J. Stat. Mech.: Theory and Exp.* (2008) P12013.
- [21] S. B. Lee and J. M. Kim, Equilibrium-restricted solid-on-solid growth model on fractal substrates, *Phys. Rev. E* **80**, 021101 (2009).
- [22] C. Lee and S. B. Lee, Surface growth on diluted lattices by a restricted solid-on-solid model, *Phys. Rev. E* **80**, 021134 (2009).
- [23] C. Lee and S. B. Lee, Height-height correlations for surface growth on percolation networks, *Physica A* **389**, 5053 (2010).
- [24] D. H. Kim and J. M. Kim, A model of random deposition with relaxation on fractal substrates, *J. Stat. Mech.: Theory and Exp.* (2010) P08008.
- [25] S. B. Lee, H.-C. Jeong, and J. M. Kim, Restricted solid-on-solid growth model for fractal substrates, *J. Korean Phys. Soc.* **58**, 1076 (2011).
- [26] Z. Xun, Y. Zhang, Y. Li, H. Xia, D. Hao, and G. Tang, Dynamic scaling behaviors of the discrete growth models on fractal substrates, *J. Stat. Mech.: Theory and Exp.* (2012) P10014.
- [27] D. H. Kim, J. M. Kim, and D. Kang, Discrete restricted curvature model with diffusion on a fractal substrate, *J. Stat. Mech.: Theory and Exp.* (2014) P07025.
- [28] G. Zumofen, J. Klafter, and A. Blumen, Langevin approach to interface statistics and diffusion-limited reactions, *Phys. Rev. A* **45**, 8977 (1992); G. Poupart and G. Zumofen, Time-dependent gradients of growing interfaces, *Phys. Rev. E* **50**, R663 (1994).
- [29] S. Havlin and D. Ben-Avraham, Diffusion on disordered media, *Adv. Phys.* **51**, 187 (2002).
- [30] A. B. Harris, Effect of random defects on the critical behavior of Ising models, *J. Phys. C* **7**, 1671 (1974).
- [31] J. Hoshen and R. Kopelman, Percolation and cluster distribution. I. Cluster multiple labeling technique and critical concentration algorithm, *Phys. Rev. B* **14**, 3438 (1976).
- [32] R. Roux and A. Hansen, A new algorithm to extract the backbone in a random resistor network, *J. Phys. A* **20**, L1281 (1987).
- [33] R. M. Ziff and B. Sapoval, The efficient determination of the percolation threshold by a frontier-generating walk in a gradient, *J. Phys. A* **19**, L1169 (1986).
- [34] D. Stauffer and A. Aharony, *Introduction to Percolation Theory* (Taylor & Francis, London, 1992).
- [35] M. D. Rintoul and H. Nakanishi, A precise determination of the backbone fractal dimension on two-dimensional percolation clusters, *J. Phys. A* **25**, L945 (1992).
- [36] P. Grassberger, A precise determination of the backbone fractal dimension on two-dimensional percolation clusters, *J. Phys. A* **25**, 5475 (1992).
- [37] S. Alexander and R. Orbach, Density of states on fractals : \ll fractons \gg , *J. Phys. (Paris) Lett.* **43**, L625 (1982).
- [38] S. B. Lee, Correction-to-scaling of random walks in disordered media, *Int. J. Mod. Phys. B* **17**, 4867 (2003).
- [39] S. B. Lee and H. Nakanishi, Self-avoiding walks on randomly diluted lattices, *Phys. Rev. Lett.* **61**, 2022 (1988).
- [40] Y. Meir and A. B. Harris, Self-avoiding walks on diluted networks, *Phys. Rev. Lett.* **63**, 2819 (1989).
- [41] B. Derrida and J. Vannimenus, A transfer-matrix approach to random resistor networks, *J. Phys. A* **15**, L557 (1982).
- [42] D. C. Hong, S. Havlin, H. J. Herrmann, and H. E. Stanley, Breakdown of Alexander-Orbach conjecture for percolation: Exact enumeration of random walks on percolation backbones, *Phys. Rev. B* **30**, 4083 (1984).
- [43] D. W. Heermann and D. Stauffer, Phase diagram for three-dimensional correlated site-bond percolation, *Z. Phys. B* **44**, 339 (1981).